A numerical study of wave propagation in a confined mixing layer by eigenfunction expansions

Fang Q. Hu
Department of Mathematics and Statistics, Old Dominion University, Norfolk, Virginia 23529

(Received 14 October 1992; accepted 17 February 1993)

It is well known that the growth rate of instability waves of a two-dimensional free shear layer is reduced greatly at supersonic convective Mach numbers. In previous works, it has been shown that new wave modes exist when the shear layers are bounded by a channel due to the coupling effect between the acoustic wave modes and the motion of the mixing layer. The present work studies the simultaneous propagation of multiple stability waves using numerical simulation. It is shown here that the coexistence of two wave modes in the flow field can lead to an oscillatory growth of disturbance energy with each individual wave mode propagating linearly. This is particularly important when the growth rates of the unstable waves are small. It is also shown here that the propagation of two neutrally stable wave modes can lead to a stationary periodic structure of rms fluctuations. In the numerical simulations presented here the forced wave modes are propagating at same frequency, but with different phase velocities. In order to track the growth of each wave mode as it propagates downstream, a numerical method that can effectively detect and separate the contribution of the individual wave is given. It is demonstrated that by a least square fitting of the disturbance field with eigenfunctions the amplitude of each wave mode can be found. Satisfactory results as compared to linear theory are obtained.

I. INTRODUCTION

In this paper we present results of numerical simulations of a confined supersonic mixing layer (Fig. 1). It is well known that at high supersonic convective Mach numbers (Mach number in the reference frame of the large-scale structure), the familiar Kelvin–Helmholtz instability wave of a free mixing layer becomes stabilized due to the increased compressibility of the flow. It was found in recent experiments,[1–3] as well as in numerical simulations,[4–6] that the spreading rate of a mixing layer at a supersonic convective Mach number is a factor of 4 or 5 smaller than at a low subsonic convective Mach number. As a result, large-scale rollups of the vorticity layer, a standard feature of low-speed free shear layers, are absent and the mixing of the two streams is inefficient. In efforts to explain these observations, a number of recent studies on the stability of the free shear layer using inviscid quasiparallel linear theory have been carried out.[7,8] These studies showed that the intrinsic instability wave of the shear layers has a much reduced growth rate when the convective Mach number becomes supersonic. It was suggested that this reduction of the unstable wave growth is directly responsible for the small spreading rate of the supersonic mixing layers observed in the experiments and direct numerical simulations.

At the same time, it was also found that a bounded free shear layer behaves differently from an unbounded one at high supersonic convective Mach numbers.[9–11] These studies revealed that the same shear layer, when bounded by a channel consisting of flat walls at the top and bottom, supports new instabilities due to the coupling between the acoustic wave modes of the channel and the motion of the shear layer. A thorough treatment of normal modes associated with a bounded shear layer was given by Tam and Hu.[9] Systematic calculations of normal mode solutions showed that four families of waves exist. In their naming convention, class A and class B modes are the unstable waves. Class A waves are related to the wave reflections from the lower wall and class B waves are related to the reflections from the upper wall. In addition, there are two families of neutrally stable waves. They were called class C and class D acoustic waves since they are related to the acoustic reflection off both walls. Typical dispersion relations of the four waves and the growth rates of A and B waves are given in Fig. 2, where the calculations have been made for two-dimensional waves at M_1 (Mach number of the upper stream) $=3.5$, M_2 (Mach number of the lower stream) $=1.2$, and the sound speeds ratio of the two streams $a_1/a_2=1.2$. In Fig. 2 a subscript has been used to indicate the corresponding mode number. It is to be noted that although the D waves have negative phase velocities, all waves have positive group velocities and hence are downstream propagating waves.

When disturbances are initiated upstream, it is expected that the wave with the largest growth rate dominates downstream. Observation of the spatial growth rates of the A and B waves indicate that at certain frequencies the A waves are dominant, while at other frequencies the B waves are the dominant waves. Yet the A and B waves have comparable growth rates. In numerical simulations, unless the upstream perturbation is an eigenfunction of a single wave mode, it is likely that both the A and B unstable waves as well as the neutrally stable waves are excited and propagate downstream. Consequently, simulations of a bounded mixing layer could be significantly different from the unbounded counterpart in two respects. First, since the A and B waves have a comparable growth rate, both waves

 0899-8213/93/061420-07$06.00 © 1993 American Institute of Physics

Reuse of AIP Publishing content is subject to the terms at: https://publishing.aip.org/authors/rights-and-permissions. Download to IP: 128.82.15.135 On: Sun, 28 Aug 2016 19:41:54

are important in downstream propagation. Second, because the growth rates of the unstable A and B waves are generally small at high convective Mach numbers, no large scale vorticity roll-ups are present, and, as a result, the excited neutrally stable waves may also constitute an important part in the downstream flow field.

The present work is concerned with the cases when multiple waves are forced at the same frequency. One objective of this paper is to show that the coexistence of multiple propagating waves can lead to an appearance of oscillatory growth of the disturbance flow field, even though the waves are growing linearly. A second objective of this paper is to construct a numerical method that can detect the growth of individual waves as they propagate.

In many experimental and computational studies it is essential to know the growth or decay rate of the propagating waves. For example, in the studies of turbulent transitions of plane mixing layers,[12,13] the spatial evolutions of the fundamental and subharmonic waves are monitored as the waves propagate downstream. The interplay of the fundamental and subharmonic waves is studied by their growth and saturation as they propagate. Usually the waves are identified by their frequencies using time series spectrum analysis of the disturbances at chosen downstream locations. The assumption is that, for plane mixing layers, the only dominant growing (unstable) wave mode is the Kelvin–Helmholtz (KH) wave. Thus the frequency spectrum naturally indicates the strength of the KH wave at any given frequency. For this reason, the local wave number of the disturbances can also be estimated from the phase difference of simultaneous measurements of the time series at two nearby points in space.[13] In this way the dispersion relationship can be established experimentally. However, when multiple wave modes of comparable strength are propagating at the same frequency but with different phase velocities, the growth or decay of each individual wave mode cannot be distinguished from an examination of the frequency spectrum alone. One method of tracking each wave is to use a cross-bispectrum analysis.[13] In this paper a method based on the eigenfunction expansion is proposed. It is shown numerically that by an expansion of the disturbances in the form of eigenfunctions it is possible to track and separate the growth of each individual mode.

In Sec. II we give the formulation of the problem and a description of the numerical methods. The method of eigenfunction expansion for detecting wave amplitudes is also described. In Sec. III results of numerical simulations and eigenfunction expansions are presented. Two cases are considered and discussed. Section IV contains the conclusions.

II. FORMULATION

A. Governing equations and numerical simulation

We consider a two-dimensional mixing layer formed between two streams of uniform parallel flow confined inside a channel (Fig. 1). The coordinate system is such that x is in the direction of the flow and y is in the direction perpendicular to x. The governing equations for an inviscid, compressible flow, in conservative form, can be written as

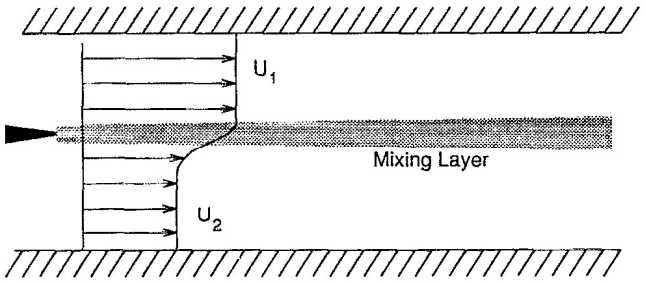

FIG. 1. Schematic drawing of a bounded shear layer.

$$\frac{\partial \mathbf{U}}{\partial t}+\frac{\partial \mathbf{E}}{\partial x}+\frac{\partial \mathbf{F}}{\partial y}=0, \tag{1}$$

where

$$\mathbf{U}=\begin{pmatrix}\rho\\ \rho u\\ \rho v\\ \rho e_t\end{pmatrix},\quad \mathbf{E}=\begin{pmatrix}\rho u\\ \rho u^2+\dfrac{p}{\gamma M_1^2}\\ \rho uv\\ \rho u e_t+\dfrac{\gamma-1}{\gamma}pu\end{pmatrix},$$

$$\mathbf{F}=\begin{pmatrix}\rho v\\ \rho uv\\ \rho v^2+\dfrac{p}{\gamma M_1^2}\\ \rho v e_t+\dfrac{\gamma-1}{\gamma}pv\end{pmatrix},$$

and $p=\rho T$, $e_t=(1/\gamma)T+[(\gamma-1)/2]M_1^2(u^2+v^2)$.

In the above equations, u and v are the velocities in the streamwise (x) and cross-stream (y) directions, respectively, ρ is the density, T is the temperature, p is the pressure, γ is the specific heats ratio, and M_1 is the upper stream Mach number. The equations have been nondimensionalized with respect to the mean velocity, temperature, and pressure of the upper stream. The height of the channel is 1. The flat walls are located at $y=-0.5$ and $y=0.5$, respectively. Boundary conditions at the walls are that v and normal derivatives of u, T, and ρ are zero.

For the purpose of this paper, an explicit second-order MacCormack scheme[14] is used to solve the above nonlinear Euler equations. Numerical solutions are advanced from time t to $t+\Delta t$ by the two-step predictor–corrector-type algorithm.

Numerical simulation starts with an initially parallel flow, namely,

$$u(x,y)=\bar{U}(y)=0.5[1+U_2+(1-U_2)\tanh(y/\delta_\omega)], \tag{2}$$

$$v(x,y)=0, \tag{3}$$

Reuse of AIP Publishing content is subject to the terms at: https://publishing.aip.org/authors/rights-and-permissions. Download to IP: 128.82.15.135 On: Sun, 28 Aug 2016 19:41:54

$$T(x,y)=\bar{T}(y)$$
$$=\left(T_2\frac{1-\bar{U}}{1-U_2}+\frac{\bar{U}-U_2}{1-U_2}+\frac{\gamma-1}{2}M_1^2(1-\bar{U})(\bar{U}-U_2)\right), \quad (4)$$

$$\rho(x,y)=\bar{\rho}(y)=\frac{1}{\bar{T}(y)}, \quad (5)$$

where δ_ω is the vorticity thickness of the mean velocity $\bar{U}(y)$. The temperature $\bar{T}(y)$ is obtained by using the Corroco's relation across the stream. Here U_2 and T_2 are the velocity and temperature of the lower stream, respectively.

To initiate the disturbances, perturbations of u, v, T, and ρ are superimposed on the mean flow at the inflow. For the computations reported here, perturbations in the form of eigenfunctions were forced. Thus the boundary values at $x=0$ are

$$\begin{pmatrix} u(0,y,t) \\ v(0,y,t) \\ T(0,y,t) \\ \rho(0,y,t) \\ p(0,y,t) \end{pmatrix} = \begin{pmatrix} \bar{U}(y) \\ 0 \\ \bar{T}(y) \\ \bar{\rho}(y) \\ 1 \end{pmatrix} + \sum_{n=1}^{N} \epsilon_n \begin{pmatrix} \hat{u}_n(y,\omega) \\ \hat{v}_n(y,\omega) \\ \hat{T}_n(y,\omega) \\ \hat{\rho}_n(y,\omega) \\ \hat{p}_n(y,\omega) \end{pmatrix} e^{-i\omega t}, \quad (6)$$

where $\hat{u}_n$, $\hat{v}_n$, $\hat{T}_n$, $\hat{\rho}_n$, and $\hat{p}_n$ are the normalized eigenfunctions of the wave modes. The normalizations are such that $|\hat{u}_n(y,\omega)|_{\max}=1$. Here N is the number of modes used in the forcing, ϵ_n is the forcing amplitude, and ω is the forcing frequency. Computations of the eigenfunctions will be briefly discussed below.

B. Eigenfuction expansion

For small perturbations forced at the inflow, the initial spatial growth is linear and is governed by the linearized Euler equations. By invoking local parallelism of the mean flow and substituting perturbations of the form $\hat{u}(y)e^{i(kx-\omega t)}$ for u and similar forms for other variables into the linearized version of (1), an eigenvalue problem for the normal modes is derived. In particular, it is found convenient to form the eigenvalue problem in the pressure perturbation. It is straightforward to determine that the equation for the pressure eigenfunction is

$$\frac{d^2\hat{p}}{dy^2}+\left(\frac{2k}{\omega-k\bar{U}}\frac{d\bar{U}}{dy}+\frac{1}{\bar{T}}\frac{d\bar{T}}{dy}\right)\frac{d\hat{p}}{dy}$$
$$+\left(\frac{(\omega-k\bar{U})^2M_1^2}{\bar{T}}-k^2\right)\hat{p}=0, \quad (7)$$

with boundary conditions $d\hat{p}/dy=0$ at $y=-0.5$ and $y=0.5$.[9] For the spatial problem considered here the frequency ω is given and the wave number k is sought from (7) as the eigenvalue. For a closed domain, the eigenvalues form a discrete set for any given ω. A typical dispersion relation of the eigenvalues is shown in Fig. 2. The corresponding $\hat{u}(y)$, $\hat{v}(y)$, $\hat{T}(y)$, and $\hat{\rho}(y)$ can be easily obtained from $\hat{p}(y)$ by using the linearized Euler equations.

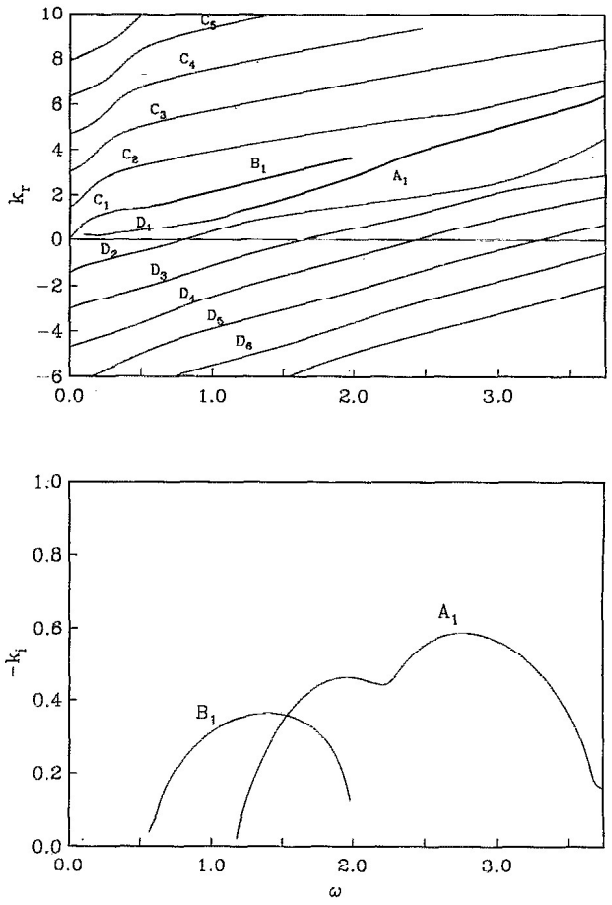

FIG. 2. Dispersion relation of the normal modes associated with a bounded supersonic shear layer. ▬, unstable modes, —, neutral modes. The mode number is denoted by subscripts. Here ω is the frequency, and k_r and k_i are the real and imaginary parts of the wave number, respectively. In addition, $M_1=3.5$, $M_2=1.2$, and $a_1/a_2=1.2$.

It is expected that the normal modes form a complete spectrum of small-amplitude waves. Indeed, for bounded flows, it was shown that eigenfunctions of hydrodynamic instability problems form a complete basis in the functional space.[15] This fact has been exploited in several recent studies, where eigenfunction expansions are used in improving numerical calculations[16] or in representing nonlinear turbulent flows.[17] Our aim here is to reconstruct the flow field obtained from the results of direct numerical simulations as a summation of eigenmodes. By doing so, the spatial development of each individual mode imposed at the inflow will be established.

To implement the expansion in eigenmodes, we first record the time series on a mesh of selected points (x_i,y_j). For convenience of discussion, let the time series of the normal velocity at (x_i,y_j) be $v'(x_i,y_j,t_n)$. Here the prime denotes the fluctuation over its mean value and t_n is the discretized time. Using a discrete FFT, the time series is transformed into the frequency spectrum, $\hat{v}'(x_i,y_j,\omega)$. We expect $\hat{v}'(x_i,y_j,\omega)$ to be a summation of eigenfunctions for fixed x_i and ω, i.e.,

$$\hat{v}'(x_i,y_j,\omega)=\sum_{n=1}^{N} a_n\hat{v}_n(y_j,\omega), \quad (8)$$

Reuse of AIP Publishing content is subject to the terms at: https://publishing.aip.org/authors/rights-and-permissions. Download to IP: 128.82.15.135 On: Sun, 28 Aug 2016 19:41:54

where $\hat{v}_n(y,\omega)$ are the eigenfunctions at frequency ω. The coefficients a_n in (8) are found by requiring that the quantity

$$E=\sum_j \left|\hat{v}'(x_i,y_j,\omega)-\sum_n a_n\hat{v}_n(y_j,\omega)\right|^2$$

be minimum. That is, the calculated time series spectrum as a function of y is fitted in the least square sense by a summation of normal mode eigenfunctions. Clearly the $\{a_n\}$ represents the wave amplitude of the corresponding mode and varies with x. It gives a measure of the strength of the wave as it propagates. For the results reported here, eigenfunction expansions are performed at the forcing frequency.

III. RESULTS AND DISCUSSIONS

To demonstrate the effects of multiple propagating wave modes and the method of eigenfunction expansion, we study two cases here. In the first case, a class B unstable wave and a class C neutrally stable wave are forced at the inflow boundary. In the second case, two neutrally stable waves, the C and D modes, are forced. In all the calculations shown here a 101×201 uniform mesh have been used for the MacCormack scheme. The computational domain extends over eight channel heights in x. The vorticity thickness of the initial flow is 0.02. The Mach number of the upper and lower stream are $M_1=3.5$ and $M_2=1.2$, respectively. The lower stream has initial velocity $U_2=0.29$ and temperature $T_2=0.91$. The two streams have a speeds of sound ratio $a_1/a_2=1.2$. The specific heats ratio $\gamma=1.4$ for both streams. The dispersion relations of the normal modes are those given in Fig. 2.

A. Case I: Simulation of B_1 and C_2 modes

The forcing modes chosen here are the B_1 and C_2 modes. The forcing amplitude is 0.015 and forcing frequency is $\omega=1$ for each mode. From linear stability calculations, the B_1 mode has a wave number of 2.13 and spatial growth rate of 0.313. The C_2 mode is a neutrally stable wave with wave number 3.93. The eigenfunctions of the two modes are shown in Fig. 3, where the velocity components $\hat{u}$ and $\hat{v}$ are plotted as functions of y.

Figure 4 shows the time series and frequency spectrum of the streamwise velocity fluctuations at selected centerline locations. At the chosen forcing level, nonlinear effects are not developed within the computational domain. A FFT was performed for the time series after $t=40$, when the initial perturbation has been "washed" out of the domain. The spectrum shows a clear peak at the forcing frequency, $\omega=1$. In Fig. 5 plots of the root-mean-square variations of velocity fluctuations across the stream are given for selected downstream locations. It is seen that the streamwise velocity has a peak in the centerline, where the shear layer is formed. However, no such peak is found in the normal velocity components. A comparison of rms fluctuations with the eigenfunctions given in Fig. 3 seems to suggest that the v components show more apparent

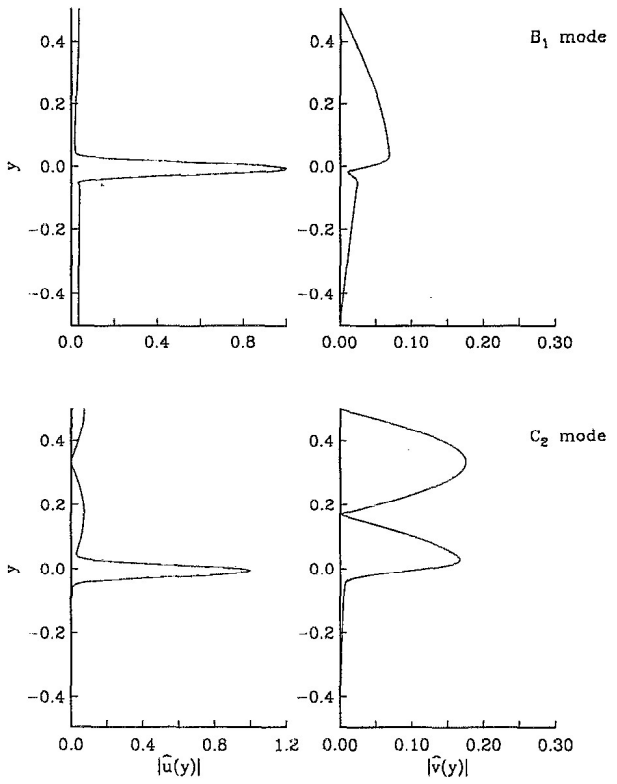

FIG. 3. Eigenfunctions of the B_1 and C_2 modes for $\omega=1$. The velocity components are shown.

modal differences than the u components. For this reason the normal velocity fluctuations are used for the eigenfunction expansion below.

As a measure of disturbance energy, we evaluate the following integral along the downstream direction:

$$\epsilon=\int_{-0.5}^{0.5}(u'^2_{\rm rms}+v'^2_{\rm rms})dy, \tag{9}$$

where $u'_{\rm rms}$ and $v'_{\rm rms}$ are the rms variations over the mean values. In Fig. 6(a), this energy integral is plotted as a function of downstream distance x. It is seen that initially the energy decreases. Farther downstream oscillatory growth is found with a period of about 3.3 channel heights. We point out that plots of maximum $u'_{\rm rms}$ or $v'_{\rm rms}$ exhibited similar trends. In Fig. 6(b), the amplitudes of B_1 and C_2 wave modes, obtained using the least square eigenfunction expansion described in Sec. II, are shown. (For the results given, time series at 51 evenly spaced y locations across the stream have been used for the least square fitting.) It is found that the growth of the B_1 wave over the downstream distance fits extremely well with a line of linear growth rate 0.313. The amplitude of the C_2 wave is shown staying more or less the same in the downstream direction. The slight variations of the C_2 amplitude are due to the accuracy limitation of the least square fitting. Figure 6(b) indicates that, although the disturbance energy in rms measurements shows oscillatory growth, each wave initiated upstream is still propagating linearly. Clearly the coexistence of the two waves leads to periodic cancellation and reinforcement, which results in the appearance of oscillatory

Reuse of AIP Publishing content is subject to the terms at: https://publishing.aip.org/authors/rights-and-permissions. Download to IP: 128.82.15.135 On: Sun, 28 Aug 2016 19:41:54

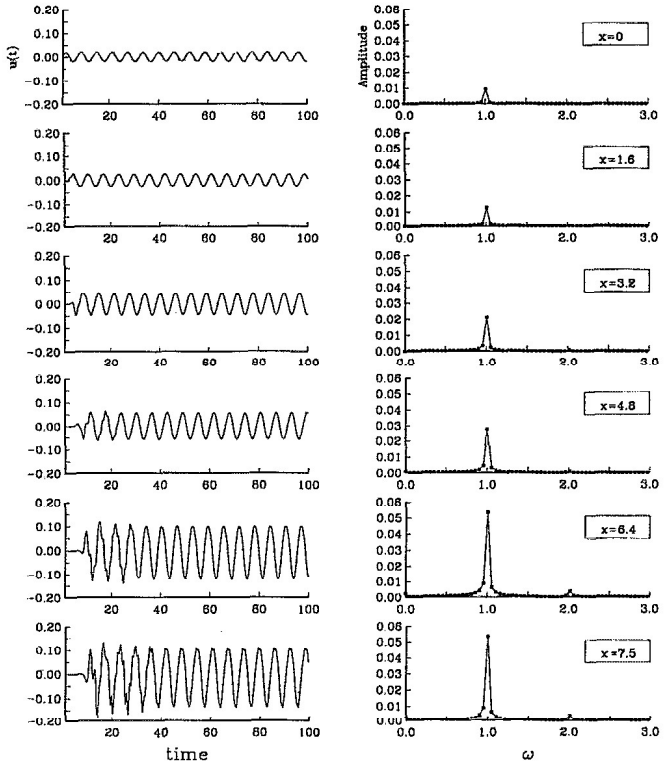

FIG. 4. The time series and spectrum at indicated centerline locations. Plotted are the streamwise velocity fluctuations. Here the B_1 and C_2 modes are forced at the inflow.

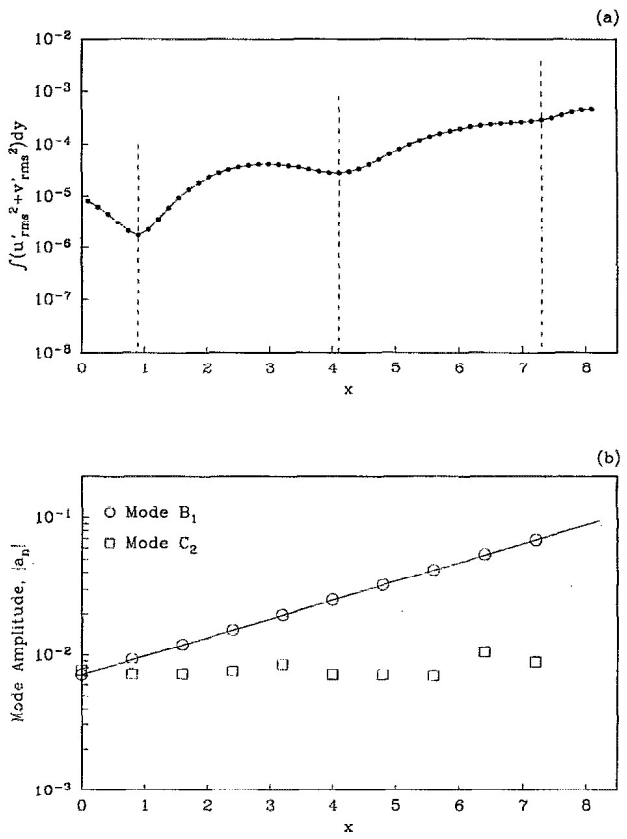

FIG. 6. (a) Energy integral (9) as a function of downstream distance x, showing oscillatory growth. Vertical dotted lines have a separation distance of 3.3. (b) Amplitudes of B_1 and C_2 modes calculated using the least square fitting with eigenfunctions. The solid straight line represents an exponential growth rate of 0.313.

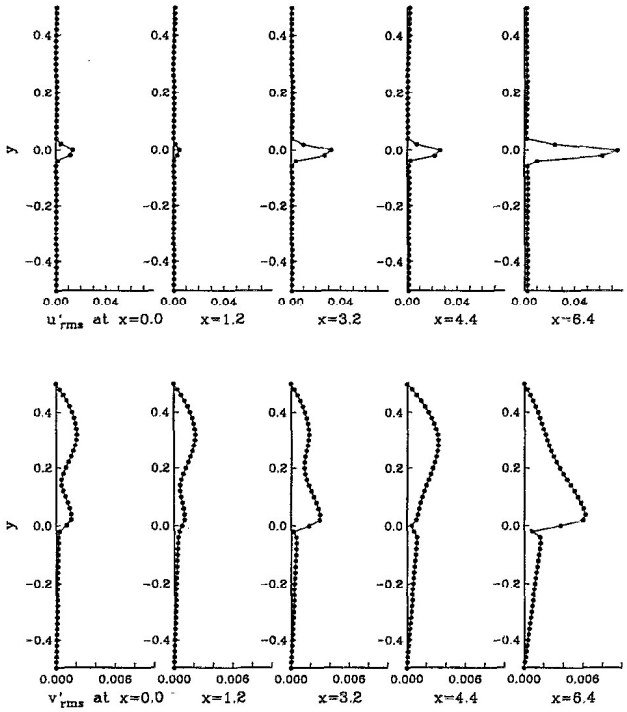

FIG. 5. Root-mean-square variations across the stream at indicated downstream locations. The velocity components are shown. Here the B_1 and C_2 modes are forced at the inflow.

growth of the energy. Similar calculations for class A waves and neutral waves have also been carried out. However, since the A waves have larger growth rates, the oscillatory behavior is not as pronounced as that shown in Fig. 6.

As pointed out in the Introduction, multiple wave modes are excited unless the disturbance at the inflow is exactly that of the eigenfunction of the chosen wave mode. The later condition is usually difficult to meet in experiments and sometimes not always imposed in numerical simulations. For example, Lu and Wu[4] used only the pressure perturbation in the inflow in their simulations. Often in experiments, the initial disturbances are excited by random fluctuations[13] or "v-component-producing" element.[18] In those studies, however, the growth rate of the unstable wave is relatively large. Because of this, the component of the unstable wave grows quickly and becomes dominant over other wave components within a short distance. As a result, a linear growth rate in disturbance energy is observed. However, as shown in the present calculations, when the growth rate of the linear instability wave is relatively small, the other excited waves can play a part in the flow field and lead to an appearance of oscillatory growth of the disturbance energy.

Reuse of AIP Publishing content is subject to the terms at: https://publishing.aip.org/authors/rights-and-permissions. Download to IP: 128.82.15.135 On: Sun, 28 Aug 2016 19:41:54

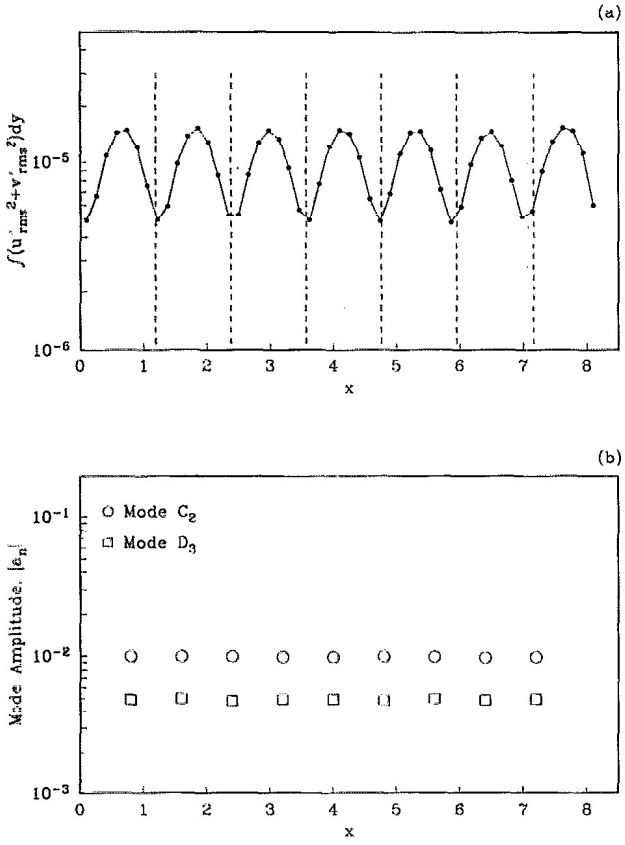

FIG. 7. (a) Energy integral (9) as a function of downstream distance x. The C_2 and D_3 modes were forced. Vertical dotted lines have separation distance of 1.19. (b) Amplitudes of the C_2 and D_3 modes calculated using least square fitting with eigenfunctions.

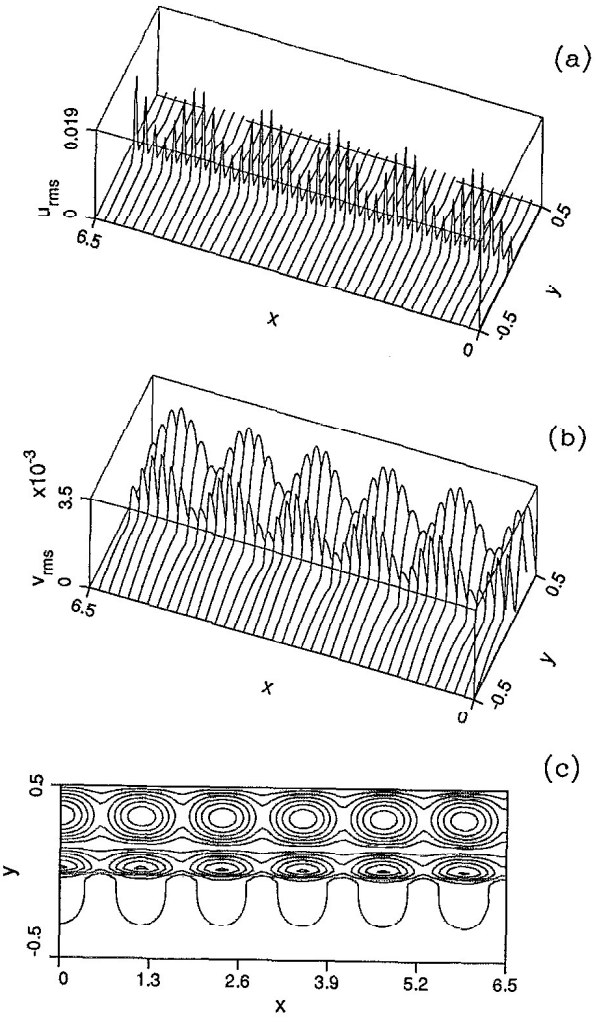

FIG. 8. Root-mean-square fluctuation as a function of x and y. (a) Streamwise velocity component; (b) normal velocity component; (c) contours of the normal velocity component shown in (b).

B. Case II: simulation of C_2 and D_3 modes

Here we study the case when two neutral modes are excited. The forcing modes are the C_2 and D_3 modes. The forcing frequency $\omega=0.25$. The wave numbers of the C_2 and D_3 modes are 2.76 and -2.53, respectively. The forcing amplitudes are 0.02 for the C_2 mode and 0.01 for the D_3 mode.

In Fig. 7(a) the resulting energy integral (9) as a function of downstream distance x is given. Using the least square eigenfunction expansion, the amplitude of each wave is calculated and given in Fig. 7(b). Figure 7 demonstrates that, although the energy of the perturbation field has a spatial periodicity, the amplitude of each wave still remains the same as they propagate downstream. Again, this is not too surprising because the two waves are traveling at different phase velocities and amplitude modulation is expected. However, it is important to note that the periodic structure of disturbance energy variation is time independent. This point is made clearer in Fig. 8, where the rms variation across the stream for u' and v' are plotted along the downstream distance. It shows that, when averaged in time, the coexistence of the C_2 and D_3 waves produces a spatially periodic and stationary structure.

The period of the structure can be estimated as below. Without the loss of generality, let two waves be $C\cos(k_C x-\omega t)$ and $D\cos(k_D x-\omega t)$, where k_C, k_D represent the wave numbers and C, D are the amplitudes. Then the mean square variation produced by the two waves is (the overbar denotes time averaging)

$$\begin{aligned}&\overline{[C\cos(k_C x-\omega t)+D\cos(k_D x-\omega t)]^2}\\&=\overline{C^2\cos^2(k_C x-\omega t)}\\&\quad+\overline{2CD\cos(k_C x-\omega t)\cos(k_D x-\omega t)}\\&\quad+\overline{D^2\cos^2(k_D x-\omega t)}\\&=\tfrac{1}{2}C^2+\tfrac{1}{2}D^2+CD\cos[(k_C-k_D)x].\end{aligned}\tag{10}$$

It is seen that a streamwise modulation is resulted with a spatial period of $2\pi/(k_C-k_D)$. This expression gives a period of 1.19 for the present case, which is the same as that observed in Figs. 7 and 8. In case I, the expression gives a period of 3.49 by substituting D by B_1 in (10).

Reuse of AIP Publishing content is subject to the terms at: https://publishing.aip.org/authors/rights-and-permissions. Download to IP: 128.82.15.135 On: Sun, 28 Aug 2016 19:41:54

IV. CONCLUSION

One difference between the numerical simulation of bounded and unbounded shear layers is that the former permits multiple propagating wave modes. This becomes important when the growth rates of the unstable waves are small. It was shown here that two forced modes can produce oscillatory growth in disturbance energy, even though each individual mode is propagating linearly. In particular, it was shown that two excited neutral modes with different phase velocities can lead to a stationary and periodic structure of the rms fluctuations. Moreover, a method of effectively detecting and separating the growth of each individual wave mode is given. Finally, it was shown numerically that, by fitting the disturbance field as a summation of eigenfunctions, the amplitude of each mode can be accurately monitored.

ACKNOWLEDGMENTS

The author wishes to thank Dr. C. E. Grosch and Dr. T. L. Jackson for helpful discussions.

This work was supported in part by the National Aeronautics and Space Administration under NASA Contract No. NAS1-19480 while the author was in residence at the Institute for Computer Applications in Science and Engineering, NASA Langley Research Center, Hampton, VA 23665.

[1]D. Papamoschou and A. Roshko, "The compressible turbulent shear layer: An experimental study," J. Fluid Mech. **197**, 453 (1988).
[2]N. T. Clemens and M. G. Mungal, "A planar Mie scattering technique for visualizing supersonic mixing flows," Exp. Fluids **11**, 175 (1991).
[3]M. Samimy and G. S. Elliott, "Effects of compressibility on the characteristics of free shear layers," AIAA J. **28**, 439 (1990).
[4]P. J. Lu and K. C. Wu, "Numerical investigation on the structure of a confined supersonic mixing layer," Phys. Fluids A **3**, 3063 (1991).
[5]P. J. Morris, M. G. Giridharan, and G. M. Lilley, "On the turbulent mixing of compressible free shear layers," Proc. R. Soc. London Ser. A **431**, 219 (1990).
[6]S. A. Ragab and S. Sheen, "Numerical simulation of a compressible mixing layer," AIAA Paper, No. 90-1669.
[7]S. A. Ragab and J. L. Wu, "Linear instability waves in supersonic turbulent mixing layers," AIAA Paper No. 87-1418, 1987.
[8]T. L. Jackson and C. E. Grosch, "Inviscid spatial stability of a compressible mixing layer," J. Fluid Mech. **208**, 609 (1989).
[9]C. K. W. Tam and F. Q. Hu, "The instability and acoustic waves of supersonic mixing layers inside a rectangular channel," J. Fluid Mech. **203**, 51 (1989).
[10]M. Zhuang, T. Kubota, and P. E. Dimotakis, "The effects of walls on a spatially growing supersonic shear layer," Phys. Fluids A **2**, 599 (1990).
[11]L. M. Mack, "On the inviscid acoustic-mode instability of supersonic shear flows, Part 1: Two-dimensional waves," Theor. Comput. Fluid Dyn. 2, 97 (1990).
[12]C. M. Ho and L. S. Huang, "Subharmonic and vortex merging in mixing layers," J. Fluid Mech. **119**, 443 (1982).
[13]M. R. Hajj, R. W. Miksad, and E. J. Powers, "Subharmonic growth by parametric resonance," J. Fluid Mech. **236**, 385 (1992).
[14]R. W. MacCormack, "Current status of numerical solutions of the Navier–Stokes equations," AIAA Paper No. 85-0032, 1985.
[15]R. C. DiPrima and G. J. Habetler, "A completeness theorem for non-self-adjoint eigenvalue problems in hydrodynamic stability," Arch. Rat. Mech. Anal. **32**, 218 (1969).
[16]M. Selmi, R. Li, and Th. Herbert, "Eigenfunction expansion of the flow in a spinning and nutating cylinder," Phys. Fluids **4**, 1998 (1992).
[17]D. S. Henningson and P. J. Schmid, "Vector eigenfunction expansion for plane channel flows," Stud. Appl. Math. **87**, 15 (1990).
[18]T. C. Corke, J. D. Krull, and M. Ghassemi, "Three-dimensional-mode resonance in far wakes," J. Fluid Mech. **239**, 99 (1992).

Reuse of AIP Publishing content is subject to the terms at: https://publishing.aip.org/authors/rights-and-permissions. Download to IP: 128.82.15.135 On: Sun, 28 Aug 2016 19:41:54